Reconstructing fine details of small objects by using plasmonic spectroscopic data. Part II: The strong interaction regime

Citation for published version:
Ammari, H, Ruiz, M, Yu, S & Zhang, H 2018, 'Reconstructing fine details of small objects by using plasmonic spectroscopic data. Part II: The strong interaction regime', *Siam journal on imaging sciences*, vol. 11, no. 3, pp. 1931–1953. https://doi.org/10.1137/17M1159877

Digital Object Identifier (DOI):
10.1137/17M1159877

Document Version:
Publisher's PDF, also known as Version of record

Published In:
Siam journal on imaging sciences

SIAM J. IMAGING SCIENCES
Vol. 11, No. 3, pp. 1931–1953

Reconstructing Fine Details of Small Objects by Using Plasmonic Spectroscopic Data. Part II: The Strong Interaction Regime*

Habib Ammari†, Matias Ruiz‡, Sanghyeon Yu†, and Hai Zhang§

Abstract. This paper is concerned with the inverse problem of reconstructing a small object from far-field measurements by using the field interaction with a plasmonic particle which can be viewed as a passive sensor. It is a follow-up of the work [H. Ammari et al., *SIAM J. Imaging Sci.*, 11 (2018), pp. 1–23], where the intermediate interaction regime was considered. In that regime, it was shown that the presence of the target object induces small shifts to the resonant frequencies of the plasmonic particle. These shifts, which can be determined from the far-field data, encode the contracted generalized polarization tensors of the target object, from which one can perform reconstruction beyond the usual resolution limit. The main argument is based on perturbation theory. However, the same argument is no longer applicable in the strong interaction regime as considered in this paper due to the large shift induced by strong field interaction between the particles. We develop a novel technique based on conformal mapping theory to overcome this difficulty. The key is to design a conformal mapping which transforms the two-particle system into a shell-core structure, in which the inner dielectric core corresponds to the target object. We show that a perturbation argument can be used to analyze the shift in the resonant frequencies due to the presence of the inner dielectric core. This shift also encodes information of the contracted polarization tensors of the core, from which one can reconstruct its shape, and hence the target object. Our theoretical findings are supplemented by a variety of numerical results based on an efficient optimal control algorithm. The results of this paper make the mathematical foundation for plasmonic sensing complete.

Key words. plasmonic sensing, superresolution, far-field measurement, generalized polarization tensors

AMS subject classifications. 35R30, 35C20

DOI. 10.1137/17M1159877

1. Introduction.

The inverse problem of reconstructing fine details of small objects by using far-field measurements is severally ill-posed. There are two fundamental reasons for this: the diffraction limit and the low signal-to-noise ratio in the measurements.

Motivated by plasmonic sensing in molecular biology (see [14] and the references therein), we developed a new methodology to overcome the ill-posedness of this inverse problem in [9]. The key idea is to use a plasmonic particle, which will be defined later, to interact with the target object and to propagate its near-field information into the far field in terms of

*Received by the editors December 5, 2017; accepted for publication (in revised form) May 30, 2018; published electronically August 9, 2018.
http://www.siam.org/journals/siims/11-3/M115987.html
Funding: The work of the third author was supported by HK RGC grant ECS 26301016 and startup fund R9355 from HKUST.
†Department of Mathematics, ETH Zürich, CH-8092 Zürich, Switzerland (habib.ammari@math.ethz.ch, sanghyeon.yu@sam.math.ethz.ch).
‡Department of Mathematics and Applications, Ecole Normale Supérieure, 75005 Paris, France (matias.ruiz@ens.fr).
§Department of Mathematics, HKUST, Clear Water Bay, Kowloon, Hong Kong (haizhang@ust.hk).

the shifts in the plasmonic resonant frequencies. This plasmonic particle can be viewed as a passive sensor in the simplest form. For such a plasmonic-particle sensor, one of the most important characterizations is the plasmonic resonant frequencies associated with it. These resonant frequencies depend not only on the electromagnetic properties of the particle and its size and shape [7, 8, 18, 25], but also on the electromagnetic properties of the environment [7, 18, 21]. It is the last property which enables the sensing application of plasmonic particles.

In [9], the target object is modeled by a dielectric particle whose size is much smaller than that of the sensing plasmonic particle. The intermediate regime where the distance of the two particles is comparable to the size of the plasmonic particle was investigated. It was shown that the shifts of the plasmonic resonant frequencies of the plasmonic particle are small and a perturbation argument can be used to derive their asymptotics. Based on these asymptotic formulas, one can obtain their explicit dependence on the generalized polarization tensors of the target particle from which one can perform its reconstruction. However, when the distance between the particles decreases, their interactions increase, and the induced shifts increase in magnitude as well. The perturbation argument will cease to work at a certain threshold distance, and the characterization for the shifts of resonant frequencies in terms of information of the target particle becomes more complicated.

In this paper, we aim to extend the above investigation to the strong interaction regime where the distance between the two particles is comparable to the size of the small particle. In this regime, the near-field interactions are strong and the induced large shifts in plasmonic resonant frequencies cannot be analyzed by a perturbation argument. In order to overcome this difficulty, we develop a novel technique based on conforming mapping theory. The key is to design a conformal mapping which transforms the two-particle system into a shell-core structure, in which the inner dielectric core corresponds to the target object. We showed that a perturbation argument can be used to analyze the shift in the resonance frequencies due to the presence of the inner dielectric core. This shift also encodes information on the contracted polarization tensors of the core, from which one can reconstruct its shape, and hence the target object. The results of this paper make the mathematical foundation for plasmonic sensing complete.

The conformal mapping technique has been applied to analyze singular plasmonic systems [22, 23]. The nearly touching or touching plasmonic-particle system exhibits strong field enhancements and shift of the resonances. The inversion mapping which is conformal was used to transform two circular disks or spheres into more symmetric systems [16, 24, 27]. After the transformation, the problems become easier to solve. We also refer the reader to [17] for the fundamental limits of the field enhancements. For the general-shaped plasmonic particles, the strong shift of the plasmonic resonances was analyzed in [15].

We remark that the above idea of plasmonic sensing is closely related to that of superresolution in resonant media, where the basic idea is to propagate the near-field information into the far field through certain near-field coupling with subwavelength resonators. In a recent series of papers [10, 11, 12], we have shown mathematically how to realize this idea by using weakly coupled subwavelength resonators and achieve superresolution and superfocusing. The key is that the near-field information of sources can be encoded in the subwavelength resonant modes of the system of resonators through the near-field coupling. These excited resonant modes can propagate into the far field, thus making the superresolution from far-field measurements possible.

This paper is organized as follows. In section 2, we provide basic results on layer potentials and then explain the concept of plasmonic resonances and the (contracted) generalized polarization tensors. In section 3, we consider the forward scattering problem of the incident field interaction with a system composed of a dielectric particle and a plasmonic particle. We derive the asymptotic of the scattered field in the case of strong regime. In section 4, we consider the inverse problem of reconstructing the geometry of the dielectric particle. This is done by constructing the contracted generalized polarization tensors of the target particle through the resonance shifts induced to the plasmonic particle. We provide numerical examples to justify our theoretical results and to illustrate the performance of the proposed optimal control reconstruction scheme.

2. Preliminaries.

2.1. Layer potentials. We denote by $G(x,y)$ the fundamental solution to the Laplacian in the free space $\mathbb{R}^2$, i.e.,

$$G(x,y) = \frac{1}{2\pi}\log|x-y|.$$

Let D be a domain $\mathbb{R}^2$ with $\mathcal{C}^{1,\eta}$ boundary for some $\eta > 0$, and let $\nu(x)$ be the outward normal for $x \in \partial D$.

We define the single-layer potential $\mathcal{S}_D$ by

$$\mathcal{S}_D[\varphi](x) = \int_{\partial D} G(x,y)\varphi(y)d\sigma(y), \quad x \in \mathbb{R}^2,$$

and the Neumann–Poincaré (NP) operator $\mathcal{K}_D^*$ by

$$\mathcal{K}_D^*[\varphi](x) = \int_{\partial D} \frac{\partial G}{\partial \nu(x)}(x,y)\varphi(y)d\sigma(y), \quad x \in \partial D.$$

The following jump relations hold:

$$\mathcal{S}_D[\varphi]\big|_+ = \mathcal{S}_D[\varphi]\big|_-, \tag{2.1}$$

$$\frac{\partial \mathcal{S}_D[\varphi]}{\partial \nu}\Big|_\pm = \Big(\pm\frac{1}{2}I + \mathcal{K}_D^*\Big)[\varphi]. \tag{2.2}$$

Here, the subscripts $+$ and $-$ indicate the limits from outside and inside D, respectively.

Let $H^{1/2}(\partial D)$ be the usual Sobolev space, and let $H^{-1/2}(\partial D)$ be its dual space with respect to the duality pairing $(\cdot,\cdot)_{-\frac{1}{2},\frac{1}{2}}$. We denote by $H_0^{-1/2}(\partial D)$ the collection of all $\varphi \in H^{-1/2}(\partial D)$ such that $(\varphi,1)_{-\frac{1}{2},\frac{1}{2}} = 0$.

The NP operator is bounded from $H^{-1/2}(\partial D)$ to $H^{-1/2}(\partial D)$. Moreover, the operator $\lambda I - \mathcal{K}_D^* : L^2(\partial D) \to L^2(\partial D)$ is invertible for any $|\lambda| > 1/2$. Although the NP operator is not self-adjoint on $L^2(\partial D)$, it can be symmetrized on $H_0^{-1/2}(\partial D)$ with a proper inner product [13, 7]. In fact, let $\mathcal{H}^*(\partial D)$ be the space $H_0^{-1/2}(\partial D)$ equipped with the inner product $(\cdot,\cdot)_{\mathcal{H}^*(\partial D)}$ defined by

$$(\varphi,\psi)_{\mathcal{H}^*(\partial D)} = -(\varphi, \mathcal{S}_D[\psi])_{-\frac{1}{2},\frac{1}{2}}$$

for $\varphi, \psi \in H^{-1/2}(\partial D)$. Then using the Plemelj's symmetrization principle,

$$\mathcal{S}_D \mathcal{K}_D^* = \mathcal{K}_D \mathcal{S}_D,$$

it can be shown that the NP operator $\mathcal{K}_D^*$ is self-adjoint in $\mathcal{H}^*$ with the inner product $(\cdot,\cdot)_{\mathcal{H}^*(\partial D)}$. It is also known that $\mathcal{K}_D^*$ is compact when the boundary ∂D is $C^{1,\eta}$ [13]. So it admits the following spectral decomposition in $\mathcal{H}^*$:

$$\mathcal{K}_D^* = \sum_{j=1}^{\infty} \lambda_j (\cdot, \varphi_j)_{\mathcal{H}^*} \varphi_j, \tag{2.3}$$

where λ_j are the eigenvalues of $\mathcal{K}_D^*$ and φ_j are their associated eigenfunctions. Note that the eigenvalues $|\lambda_j| < 1/2$ for all $j \geq 1$.

2.2. Electromagnetic scattering in the quasi-static approximation. Let us consider a particle D embedded in the free space $\mathbb{R}^2$. Equivalently, the particle D in $\mathbb{R}^3$ has a translational symmetry in the direction of the x_3-axis. Let ε_D (resp., ε_m) be the permittivity of the particle D (resp., of the background). So the permittivity distribution ε is given by

$$\varepsilon = \varepsilon_D \chi(D) + \varepsilon_m \chi(\mathbb{R}^2 \backslash \overline{D}),$$

where $\chi(D)$ is the characteristic function of D. We also assume the permeability distribution μ is homogeneous over the whole space, i.e., $\mu \equiv \mu_m$ in $\mathbb{R}^2$.

We are interested in the scattering of the electromagnetic fields (E, H) by the particle D satisfying

$$\begin{cases} \nabla \times E = i\omega\mu H, \\ \nabla \times H = -i\omega\varepsilon E, \end{cases}$$

where ω is the operating frequency.

We consider the TM polarization, i.e., $E = (E_1, E_2, 0)$ and $H = (0, 0, H_3)$. Then the magnetic field component H_3 satisfies the scalar Helmholtz equation as follows:

$$\left(\nabla \cdot \frac{1}{\varepsilon}\nabla + \omega^2\mu\right) H_3 = 0 \quad \text{in } \mathbb{R}^2.$$

Also, the electric field E is given by

$$E = (E_1, E_2, 0) = \frac{1}{i\omega\varepsilon}(-\partial_y H_3, \partial_x H_3, 0).$$

We suppose that the incident field $H^{inc} = (0, 0, H_3^i)$ is in the form of a plane wave:

$$H_3^i = e^{ik^i \cdot x}, \quad k^i = k_m(\sin\theta_i, -\cos\theta_i),$$

where $k_m = \omega\sqrt{\varepsilon_m \mu_m}$ is the free space wave number and θ_i is the incident angle. Then the corresponding electric field $E^i = (E_1^i, E_2^i, 0)$ is given by

$$(E_1^i, E_2^i) = \sqrt{\frac{\mu_m}{\varepsilon_m}} e^{ik^i \cdot x}(\cos\theta_i, \sin\theta_i).$$

We assume that the particle D is small compared to the wavelength of the incident wave. Then we can adopt the quasi-static approximation, and the electromagnetic scattering can be described by a scalar function u, which is called the electric potential. We suppose that the domain of the particle D contains the origin for simplicity. In the vicinity of the particle D, the electric field $E = (E_1, E_2, 0)$ is approximated as

$$(E_1, E_2) \approx -\nabla u,$$

and the electric potential u satisfies

$$\begin{cases} \nabla \cdot (\varepsilon \nabla u) = 0 & \text{in } \mathbb{R}^2, \\ u - u^i = O(|x|^{-1}) & \text{as } |x| \to \infty, \end{cases} \tag{2.4}$$

where u^i means the electric potential of the incident field given by

$$u^i = -\sqrt{\frac{\mu_m}{\varepsilon_m}}(\cos\theta_i, \sin\theta_i) \cdot x.$$

It is worth mentioning that in the quasi-static approximation, H_3 satisfies $\nabla \cdot (1/\varepsilon)\nabla H_3 = 0$. So H_3 also plays a similar role to the potential u. In fact, one can check that H_3 is a harmonic conjugate of the potential u up to a multiplicative constant [19]. We choose the potential u to describe the scattering since its gradient directly gives the electric field E.

The electric potential u can be represented as (see, for example, [13])

$$u = u^i + \mathcal{S}_D[\varphi], \tag{2.5}$$

where the density φ satisfies the boundary integral equation

$$(\lambda I - \mathcal{K}_D^*)[\varphi] = \frac{\partial u^i}{\partial \nu}\Big|_{\partial D}. \tag{2.6}$$

Here, λ is given by

$$\lambda = \frac{\varepsilon_D + \varepsilon_m}{2(\varepsilon_D - \varepsilon_m)}. \tag{2.7}$$

2.3. Contracted generalized polarization tensors. In this subsection, we review the concept of the generalized polarization tensors (GPTs). It is known that the scattered field $u - u^i$ has the following asymptotic expansion in the far field [3, p. 77]:

$$(u - u^i)(x) = \sum_{|\alpha|,|\beta|\le 1} \frac{1}{\alpha!\beta!}\partial^\alpha u^i(0) M_{\alpha\beta}(\lambda, D)\partial^\beta G(x), \quad |x| \to +\infty, \tag{2.8}$$

where $M_{\alpha\beta}(\lambda, D)$ is given by

$$M_{\alpha\beta}(\lambda, D) := \int_{\partial D} y^\beta (\lambda I - \mathcal{K}_D^*)^{-1}\left[\frac{\partial x^\alpha}{\partial \nu}\right](y)\, d\sigma(y), \qquad \alpha, \beta \in \mathbb{N}^2.$$

Here, the coefficient $M_{\alpha\beta}(\lambda, D)$ is called the *generalized polarization tensor* [3].

Next we consider the simplified version of the GPTs. For a positive integer m, let $P_m(x)$ be the complex-valued polynomial

$$P_m(x) = (x_1 + ix_2)^m = r^m \cos m\theta + ir^m \sin m\theta, \tag{2.9}$$

where we have used the polar coordinates $x = re^{i\theta}$.

We define the *contracted generalized polarization tensors* (CGPTs) to be the following linear combinations of GPTs using the polynomials in (2.9):

$$\begin{aligned} M^{cc}_{m,n}(\lambda, D) &= \int_{\partial D} \mathrm{Re}\{P_n\}(\lambda I - \mathcal{K}^*_D)^{-1}\left[\frac{\partial\,\mathrm{Re}\{P_m\}}{\partial\nu}\right] d\sigma, \\ M^{cs}_{m,n}(\lambda, D) &= \int_{\partial D} \mathrm{Im}\{P_n\}(\lambda I - \mathcal{K}^*_D)^{-1}\left[\frac{\partial\,\mathrm{Re}\{P_m\}}{\partial\nu}\right] d\sigma, \\ M^{sc}_{m,n}(\lambda, D) &= \int_{\partial D} \mathrm{Re}\{P_n\}(\lambda I - \mathcal{K}^*_D)^{-1}\left[\frac{\partial\,\mathrm{Im}\{P_m\}}{\partial\nu}\right] d\sigma, \\ M^{ss}_{m,n}(\lambda, D) &= \int_{\partial D} \mathrm{Im}\{P_n\}(\lambda I - \mathcal{K}^*_D)^{-1}\left[\frac{\partial\,\mathrm{Im}\{P_m\}}{\partial\nu}\right] d\sigma. \end{aligned} \tag{2.10}$$

We remark that the CGPTs defined above encode useful information about the shape of the particle D and can be used for its reconstruction. See [3, 2, 4, 5] for more details.

For convenience, we introduce the following notation. We denote

$$M_{m,n}(\lambda, D) = \begin{pmatrix} M^{cc}_{m,n}(\lambda, D) & M^{cs}_{m,n}(\lambda, D) \\ M^{sc}_{m,n}(\lambda, D) & M^{ss}_{m,n}(\lambda, D) \end{pmatrix}.$$

It is worth mentioning that the following symmetry holds (see [3]):

$$M_{m,n} = M^{\intercal}_{n,m},$$

where $\intercal$ stands for the transpose.

When $m = n = 1$, the matrix $M(\lambda, D) := M_{1,1}(\lambda, D)$ is called the *first order polarization tensor*. Specifically, we have

$$M(\lambda, D)_{lm} = \int_{\partial D} y_m(\lambda I - \mathcal{K}^*_D)^{-1}[\nu_l](y)\, d\sigma(y), \quad l, m = 1, 2.$$

We also have from (2.8) that

$$(u - u^i)(x) = \frac{x^{\intercal} \cdot M(\lambda, D)\nabla u^i}{|x|^2} + O(|x|^{-2}) \quad \text{as } |x| \to \infty.$$

So the leading order term in the far-field expansion of the scattered field $u - u^i$ is determined by the first order polarization tensor $M(\lambda, D)$. The quantity $M(\lambda, D)(-\nabla u^i)$ is called the dipole moment. In fact, the leading order term is the electric potential generated by a point dipole source with dipole moment $M(\lambda, D)(-\nabla u^i)$.

2.4. Plasmonic resonances. Here we explain the plasmonic resonances. We say that the particle D is plasmonic when its permittivity ε_D has a negative real part. It is known that the permittivity of noble metals, such as gold and silver, has such a property. More precisely, the permittivity ε_D of the plasmonic (or metallic) particle D is often modeled by the following Drude's model [20]:

$$\varepsilon_D = \varepsilon_D(\omega) = 1 - \frac{\omega_p^2}{\omega(\omega + i\gamma)}, \tag{2.11}$$

where ω is the operating frequency. Here, $\omega_p > 0$ denotes the plasma frequency and $\gamma > 0$ the damping parameter. Usually, the parameter γ is a very small number. So $\varepsilon_D(\omega)$ also has a small imaginary part. Note that when $\omega < \omega_p$, the permittivity ε_D has a negative real part. Contrary to plasmonic particles, ordinary dielectric particles have positive real parts. Note that, by (2.7), λ becomes frequency dependent.

Now we discuss the resonant behavior of the solution u when ε_D is negative (or the particle D is plasmonic). Recall that the solution u is represented as

$$u = u^i + \mathcal{S}_D[\varphi], \tag{2.12}$$

where the density φ satisfies the boundary integral equation

$$(\lambda(\omega)I - \mathcal{K}_D^*)[\varphi] = \frac{\partial u^i}{\partial \nu}\Big|_{\partial D}. \tag{2.13}$$

By the spectral decomposition (2.3) of $\mathcal{K}_D^*$, we have from (2.6) that

$$u = u^i + \sum_{j=1}^{\infty} \frac{(\frac{\partial u^i}{\partial \nu}, \varphi_j)_{\mathcal{H}^*(\partial D)}}{\lambda(\omega) - \lambda_j} \mathcal{S}_D[\varphi_j]. \tag{2.14}$$

Recall that λ_j are eigenvalues of $\mathcal{K}_D^*$ and they satisfy the condition that $|\lambda_j| < 1/2$. When ε_D has a negative real part, we have $|\mathrm{Re}\{\lambda(\omega)\}| < 1/2$. Let ω_j be such that $\lambda(\omega_j) = \lambda_j$. Then if ω is close to ω_j and $(\frac{\partial u^i}{\partial \nu}, \varphi_j)_{\mathcal{H}^*(\partial D)} \neq 0$, the function $\mathcal{S}_D[\varphi_j]$ in (2.14) will be greatly amplified and dominates over other terms. As a result, the magnitude of the scattered field $u - u^i$ will show a pronounced peak at the frequency ω_j as a function of the frequency ω. This phenomenon is called the plasmonic resonance, and ω_j is called the plasmonic resonant frequency and $\mathcal{S}_D[\varphi_j]$ the resonant mode.

Let us discuss how we can measure the resonant frequency ω_j or the eigenvalue λ_j from the far-field measurements. In fact, the far field for the solution $-\nabla u$ is not equal to the true far field of the electromagnetic wave since the quasi-static approximation is valid only in the vicinity of the particle D. But the polarization tensor $M(\lambda, D)$, which is introduced in the quasi-static approximation, is useful when describing the far-field behavior of the true scattered field.

We first represent $M(\lambda, D)$ in a spectral form. By (2.3), we have

$$M(\lambda, D)_{lm} = \sum_{j=1}^{\infty} \frac{(y_m, \varphi_j)_{-\frac{1}{2},\frac{1}{2}} (\varphi_j, \nu_l)_{\mathcal{H}^*(\partial D)}}{\lambda(\omega) - \lambda_j}.$$

As discussed in subsection 2.3, the small particle D can be considered as a point dipole source located at $x_0 \in \mathbb{R}^2$, and its dipole moment is given by $p_D = M(\lambda, D)(-\nabla u^i)$. We can see from the above spectral representation that the dipole moment p_D becomes resonant when $\omega \approx \omega_j$.

Let $\mathcal{G}^k$ be the dyadic Green's function

$$\mathcal{G}^k(x,y) = (k^2 I + \nabla \cdot \nabla) G^k(x,y),$$

where $G^k(x,y) = -\frac{i}{4} H_0^{(1)}(k|x-y|)$ and k is the wave number. Then the (true) scattered electric field E^s is well approximated over the whole region as [6, 26]

$$E^s \approx \mathcal{G}^{k_m}(x, x_0) p_D.$$

So, if $\omega \approx \omega_j$, then the amplitude of the scattered wave E^s will be greatly enhanced. Therefore, as a function of the frequency ω, it will have local peaks from which we can recover the resonant frequency ω_j (or the plasmonic eigenvalue λ_j). More specifically, we measure the so-called absorption cross-section σ_a from the scattered field E^s at the far-field region. In fact, this quantity can be approximated as $\sigma_a \propto \mathrm{Im}(p_D)$ for a small plasmonic particle.

3. The forward problem.

We consider a system composed of a dielectric particle and a plasmonic particle embedded in a homogeneous medium. The target dielectric particle and the plasmonic particle occupy, respectively, a bounded and simply connected domain $D_1 \subset \mathbb{R}^2$ and $D_2 \subset \mathbb{R}^2$ of class $\mathcal{C}^{1,\alpha}$ for some $0 < \alpha < 1$. We denote the permittivity of the dielectric particle D_1 and the plasmonic particle D_2 by ε_1 and ε_2, respectively. As before, the permittivity of the background medium is denoted by ε_m. So the permittivity distribution ε is given by

$$\varepsilon := \varepsilon_1 \chi(D_1) + \varepsilon_2 \chi(D_2) + \varepsilon_m \chi(\mathbb{R}^2 \setminus (\overline{D_1 \cup D_2})).$$

As in subsection 2.4, the permittivity ε_2 of the plasmonic particle D_2 depends on the operating frequency and is modeled as

$$\varepsilon_2 = \varepsilon_2(\omega) = 1 - \frac{\omega_p^2}{\omega(\omega + i\gamma)}.$$

The total electric potential u satisfies the following equation:

$$\begin{cases} \nabla \cdot (\varepsilon \nabla u) = 0 & \text{in } \mathbb{R}^2 \setminus (\partial D_1 \cup \partial D_2), \\ u|_+ = u|_- & \text{on } \partial D_1 \cup \partial D_2, \\ \varepsilon_m \dfrac{\partial u}{\partial \nu}\Big|_+ = \varepsilon_1 \dfrac{\partial u}{\partial \nu}\Big|_- & \text{on } \partial D_1, \\ (u - u^i)(x) = O(|x|^{-1}) & \text{as } |x| \to \infty, \end{cases} \tag{3.1}$$

where $u^i(x)$ is the electric potential for a given incident field as before.

3.1. Boundary integral formulation. We derive a layer potential representation of the total field u to (3.1) in this section. We first denote by u_{D_1} the total field resulting from the incident field u^i and the ordinary particle D_1 (in the absence of the plasmonic particle D_2). Let us denote

$$\lambda_{D_j} = \frac{\varepsilon_j + \varepsilon_m}{2(\varepsilon_j - \varepsilon_m)}, \quad j = 1, 2.$$

Then u_{D_1} has the following representation [3]:

$$u_{D_1}(x) = u^i(x) + \mathcal{S}_{D_1} \left(\lambda_{D_1}\mathrm{Id} - \mathcal{K}^*_{D_1}\right)^{-1} \left[\frac{\partial u^i}{\partial \nu_1}\right](x) \quad \text{ for } x \in \mathbb{R}^2 \backslash \overline{D_1}.$$

We next introduce the Green's function $G_{D_1}(\cdot, y)$ for the medium with permittivity distribution $\varepsilon_{D_1}\chi(D_1) + \varepsilon_m\chi(\mathbb{R}^2\backslash\overline{D_1})$. More precisely, $G_{D_1}(\cdot, y)$ satisfies the equation

$$\nabla_x \cdot \big((\varepsilon_{D_1}\chi(D_1) + \varepsilon_m\chi(\mathbb{R}^2\backslash\overline{D_1}))\nabla_x G_{D_1}(x, y)\big) = \delta(x - y).$$

Using G_{D_1}, we define the layer potential $\mathcal{S}_{D_2,D_1}$ by

$$\mathcal{S}_{D_2,D_1}[\varphi](x) = \int_{\partial D_2} G_{D_1}(x, y)\varphi(y)d\sigma(y).$$

We also define

$$\mathcal{A} = \mathcal{K}^*_{D_2} - \frac{\partial}{\partial \nu_2}\mathcal{S}_{D_1} \left(\lambda_{D_1}\mathrm{Id} - \mathcal{K}^*_{D_1}\right)^{-1} \frac{\partial \mathcal{S}_{D_2}[\cdot]}{\partial \nu_1}.$$

It was proved in [9] that the solution u can be represented using $\mathcal{S}_{D_2,D_1}$ and $\mathcal{A}$ as shown in the following lemma.

Lemma 3.1 (see [9]). *The total electric potential u can be represented as follows:*

$$u = u_{D_1} + \mathcal{S}_{D_2,D_1}[\psi], \quad x \in \mathbb{R}^2\backslash\overline{D_2}, \tag{3.2}$$

where the density ψ satisfies

$$\left(\lambda_{D_2}\mathrm{Id} - \mathcal{A}\right)[\psi] = \frac{\partial u_{D_1}}{\partial \nu_2}. \tag{3.3}$$

3.2. Strong interaction regime and conformal transformation. We assume the following condition on the sizes of the particles D_1 and D_2.

Condition 1. *The plasmonic particle D_2 has size of order one; the dielectric particle D_1 has size of order $\delta \ll 1$.*

Definition 3.1 (strong interaction regime). *We say that the small dielectric particle D_1 is in the strong regime with respect to the plasmonic particle D_2 if there exist positive constants C_1 and C_2 such that $C_1 < C_2$ and*

$$C_1\delta \leq \mathrm{dist}(D_1, D_2) \leq C_2\delta.$$

Definition 3.1 says that the dielectric particle D_1 is closely located to the plasmonic particle D_2 with a separation distance of order δ.

In our recent paper [9], the intermediate interaction regime is considered. The key observation is that, if we assume the distance between D_1 and D_2 is of order one, then the effect of the small unknown particle D_1 can be considered as a small perturbation. To see this, we rewrite (3.3) in the form

$$\left(\mathcal{A}_{D_2,0} + \mathcal{A}_{D_2,1}\right)[\psi] = \frac{\partial u_{D_1}}{\partial \nu_2}, \tag{3.4}$$

where

$$\begin{aligned} \mathcal{A}_{D_2,0} &= \lambda_{D_2}\mathrm{Id} - \mathcal{K}^*_{D_2}, \\ \mathcal{A}_{D_2,1} &= \frac{\partial}{\partial \nu_2}\mathcal{S}_{D_1}\left(\lambda_{D_1}\mathrm{Id} - \mathcal{K}^*_{D_1}\right)^{-1}\frac{\partial \mathcal{S}_{D_2}[\cdot]}{\partial \nu_1}. \end{aligned} \tag{3.5}$$

It can be shown that the operator $\mathcal{A}_{D_2,1}$ is a small perturbation to the operator $\mathcal{A}_{D_2,0}$ [9], and so the authors were able to apply the perturbation method for analyzing the plasmonic resonance. However, in the strong interaction regime, the operator $\mathcal{A}_{D_2,1}$ is no longer small compared to the latter. As a consequence, the perturbation theory is not applicable, and it becomes challenging to analyze the interaction between the particles.

We now introduce a method to tackle this issue by using a conformal mapping technique. Let B_1 be a circular disk containing the dielectric particle D_1 with radius r_1 of order δ. We assume the plasmonic particle D_2 is a circular disk with radius r_2. For convenience, we denote D_2 by B_2. We emphasize that the shape of D_1 is unknown. We let d be the distance between the two disks B_1 and B_2, i.e.,

$$d = \mathrm{dist}(B_1, B_2).$$

By the assumption, d is of order δ.

Let R_j be the reflection with respect to ∂B_j, and let $\mathbf{p}_1$ and $\mathbf{p}_2$ be the unique fixed points of the combined reflections $R_1 \circ R_2$ and $R_2 \circ R_1$, respectively. Let $\mathbf{n}$ be the unit vector in the direction of $\mathbf{p}_2 - \mathbf{p}_1$. We set $(x, y) \in \mathbb{R}^2$ to be the Cartesian coordinates such that $\mathbf{p} = (\mathbf{p}_1 + \mathbf{p}_2)/2$ is the origin and the x-axis is parallel to $\mathbf{n}$. Then one can see that $\mathbf{p}_1$ and $\mathbf{p}_2$ can be written as

$$\mathbf{p}_1 = (-a, 0) \quad \text{and} \quad \mathbf{p}_2 = (a, 0), \tag{3.6}$$

where the constant a is given by

$$a = \frac{\sqrt{d}\sqrt{(2r_1 + d)(2r_2 + d)(2r_1 + 2r_2 + d)}}{2(r_1 + r_2 + d)}. \tag{3.7}$$

Then the center $\mathbf{c}_i$ of B_i $(i = 1, 2)$ is given by

$$\mathbf{c}_i = \left((-1)^i\sqrt{r_i^2 + a^2}, 0\right). \tag{3.8}$$

Define the conformal transformation Φ by

$$\zeta = \Phi(z) = \frac{z+a}{z-a}, \quad z = x + iy.$$

In other words,

$$z = \Phi^{-1}(\zeta) = a\frac{\zeta+1}{\zeta-1}.$$

We also define

$$s_j = (-1)^j \sinh^{-1}(a/r_j), \quad j = 1, 2,$$

and the two disks $\widetilde{B}_1$ and $\widetilde{B}_2$ by

$$\widetilde{B}_1 = \{|\zeta| < \tilde{r}_j\}, \quad \tilde{r}_j = \exp(s_j), \ j = 1, 2.$$

It can be shown that, in the ζ-plane, the disks B_1 and B_2 are transformed to

$$\Phi(B_1) = \widetilde{B}_1 = \{|\zeta| < \tilde{r}_1\}$$

and

$$\Phi(B_2) = \mathbb{R}^2 \setminus \overline{\widetilde{B}_2} = \{|\zeta| > \tilde{r}_2\}.$$

One can check that $\tilde{r}_1 < 1$ and $\tilde{r}_2 > 1$. The exterior region $\mathbb{R}^2 \setminus \overline{B_1 \cup B_2}$ becomes a shell region between $\partial\widetilde{B}_1$ and $\partial\widetilde{B}_2$ in the ζ-plane:

$$\Phi(\mathbb{R}^2 \setminus \overline{B_1 \cup B_2}) = \widetilde{B}_2 \setminus \overline{\widetilde{B}_1} = \{\tilde{r}_1 < |\zeta| < \tilde{r}_2\}.$$

To illustrate the geometry, in Figure 1 we show an example of the configuration of a system of a small dielectric particle D_1 and a plasmonic particle B_2. We also show its transformed geometry by the conformal map Φ. We set $\delta = 0.2$, $r_1 = \delta$, $r_2 = 1$, and $d = \delta$.

It is worth mentioning that the shape of the transformed domain $\widetilde{D}_1$ strongly depends on the ratio between d and δ but is independent of δ itself. Suppose that $d = c\delta$ for some $c > 0$. If c is of order one, then the shape of $\widetilde{D}_1$ is almost the same as that of D_1. On the contrary, if c is too small, then the shape of $\widetilde{D}_1$ is highly distorted. See Figure 2.

3.3. Boundary integral formulation in the transformed domain. Let us define $\tilde{u}(\zeta) = u(\Phi^{-1}(\zeta))$ and $\tilde{u}^i(\zeta) = u^i(\Phi^{-1}(\zeta))$. Then, since the mapping Φ is conformal, $\tilde{u}$ and $\tilde{u}^i$ are harmonic in the ζ-plane. Moreover, the transmission conditions for $\tilde{u}$ are preserved. In fact, the transformed potential $\tilde{u}$ satisfies the following equations:

$$\begin{cases} \nabla \cdot (\tilde{\varepsilon} \nabla \tilde{u}) = 0 & \text{in } \mathbb{R}^2 \backslash (\partial\widetilde{D}_1 \cup \partial\widetilde{D}_2), \\ \tilde{u}|_+ = \tilde{u}|_- & \text{on } \partial\widetilde{D}_1 \cup \partial\widetilde{D}_2, \\ \varepsilon_m \dfrac{\partial \tilde{u}}{\partial \nu}\Big|_+ = \varepsilon_1 \dfrac{\partial \tilde{u}}{\partial \nu}\Big|_- & \text{on } \partial\widetilde{D}_1, \\ \varepsilon_2 \dfrac{\partial \tilde{u}}{\partial \nu}\Big|_+ = \varepsilon_m \dfrac{\partial \tilde{u}}{\partial \nu}\Big|_- & \text{on } \partial\widetilde{D}_2, \\ (\tilde{u} - \tilde{u}^i)(\zeta) = O(|\zeta - (1,0)|) & \text{as } \zeta \to (1,0), \end{cases} \tag{3.9}$$

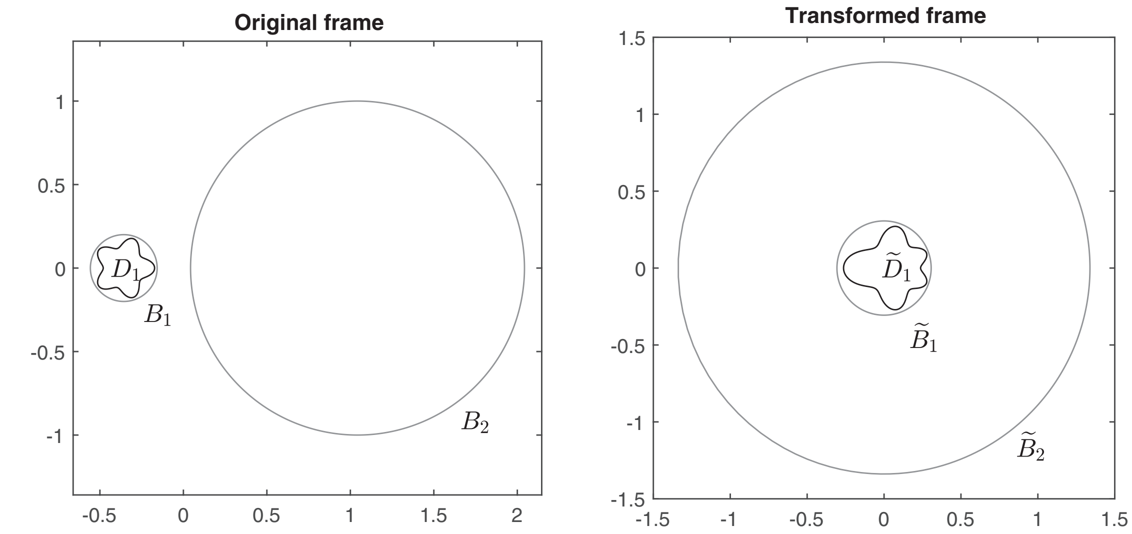

Figure 1. *Original configuration (left) and one transformed by the conformal map Φ (right).*

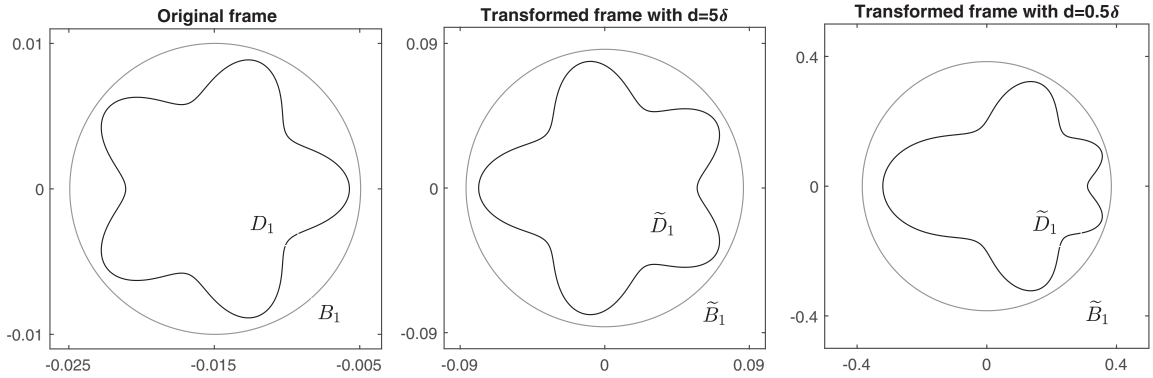

Figure 2. *Original configuration (left), the one transformed with $d = 5\delta$ (center), and the same but with $d = 0.5\delta$ (right). We set $r_1 = \delta$, $r_2 = 1$, and $\delta = 0.01$.*

where the transformed permittivity distribution $\tilde{\varepsilon}$ is given by

$$\tilde{\varepsilon} = \varepsilon_1 \chi(\widetilde{D}_1) + \varepsilon_2 \chi(\mathbb{R}^2 \setminus \widetilde{D}_2) + \varepsilon_m \chi(\widetilde{D}_2 \setminus \overline{\widetilde{D}_1}).$$

Note that the transformed problem looks similar to the original one, even though the geometry of the particles is of a completely different nature. As δ goes to zero, the radii $\tilde{r}_1$ and $\tilde{r}_2$ have the following asymptotic properties:

$$\tilde{r}_1 = \tilde{r}_1^0 + O(\delta), \quad \tilde{r}_2 = 1 + O(\delta)$$

for some $0 < r_1^0 < 1$ independent of δ. Hence, in contrast to the original problem, the transformed boundaries $\partial\widetilde{B}_1$ and $\partial\widetilde{B}_2$ $(= \partial\widetilde{D}_2)$ are not close to touching. Moreover, they share the same center (see Figure 1). This will enable us to analyze more deeply the spectral nature of the problem.

Now we represent the solution to the transformed problem using the layer potentials. By applying a procedure similar to the one used for (3.5), we can obtain the following representation:

$$\tilde{u} = (\text{const.}) + u_{\widetilde{D}_1} + \mathcal{S}_{\widetilde{D}_2,\widetilde{D}_1}[\widetilde{\psi}], \quad x \in \mathbb{R}^2. \tag{3.10}$$

Here, the constant term is needed to satisfy the last condition in (3.9). The density function $\widetilde{\psi}$ satisfies the following boundary integral equation:

$$\left(\lambda_{D_2} I - \widetilde{\mathcal{A}}\right)[\widetilde{\psi}] = \frac{\partial \tilde{u}_{\widetilde{D}_1}}{\partial \nu_2}, \tag{3.11}$$

where

$$\widetilde{\mathcal{A}} = \mathcal{K}^*_{\widetilde{D}_2} - \frac{\partial}{\partial \nu_2} \mathcal{S}_{\widetilde{D}_1} \left(\lambda_{D_1} I - \mathcal{K}^*_{\widetilde{D}_1}\right)^{-1} \frac{\partial \mathcal{S}_{\widetilde{D}_2}[\cdot]}{\partial \nu_1}, \tag{3.12}$$

$$\tilde{u}_{\widetilde{D}_1} = \tilde{u}^i + \mathcal{S}_{\widetilde{D}_1} \left(\lambda_{D_1} I - \mathcal{K}^*_{\widetilde{D}_1}\right)^{-1} \left[\frac{\partial \tilde{u}^i}{\partial \nu_1}\right]. \tag{3.13}$$

Lemma 3.2. *The following relation between $\mathcal{A}$ and $\widetilde{\mathcal{A}}$ holds:*

$$(\phi, \mathcal{A}[\psi])_{\mathcal{H}^*(\partial D_2)} = (\widetilde{\phi}, \widetilde{\mathcal{A}}[\widetilde{\psi}])_{\mathcal{H}^*(\partial \widetilde{D}_2)}, \tag{3.14}$$

where $\phi, \psi \in \mathcal{H}^*(\partial D_2)$ and $\widetilde{\phi} = \phi \circ \Phi^{-1}, \widetilde{\psi} = \psi \circ \Phi^{-1}$.

Proof. By the conformality of the map Φ, the single-layer potentials $\mathcal{S}_{D_2}[\phi]$ and $\mathcal{S}_{\widetilde{D}_2}[\widetilde{\phi}] \circ \Phi$ are identical up to an additive constant, whence (3.14) follows. ∎

3.4. Computation of the operator $\widetilde{\mathcal{A}}$ and its spectral properties. Here we compute the operator $\widetilde{\mathcal{A}}$. Note that $\widetilde{\mathcal{A}}$ is an operator which maps $\mathcal{H}^*(\partial \widetilde{D}_2)$ onto $\mathcal{H}^*(\partial \widetilde{D}_2)$. Since $\partial \widetilde{D}_2$ is a circle, we use the Fourier basis for $\mathcal{H}^*(\partial \widetilde{D}_2)$. Let (r, θ) be the polar coordinates in the ζ-plane, i.e., $\zeta = re^{i\theta}$. We define

$$\varphi^c_n(\theta) = \cos n\theta, \quad \varphi^s_n(\theta) = \sin n\theta.$$

The following proposition holds.

Proposition 3.1. *We have*

$$\widetilde{\mathcal{A}}[\varphi^c_n](\zeta) = \sum_{m=1}^{\infty} -\frac{\tilde{r}_2^{-(n+m)}}{4\pi n} \left(M^{cc}_{nm}(\lambda_{D_1}, \widetilde{D}_1) \cos m\theta + M^{cs}_{nm}(\lambda_{D_1}, \widetilde{D}_1) \sin m\theta\right) \tag{3.15}$$

and

$$\widetilde{\mathcal{A}}[\varphi^s_n](\zeta) = \sum_{m=1}^{\infty} -\frac{\tilde{r}_2^{-(n+m)}}{4\pi n} \left(M^{sc}_{nm}(\lambda_{D_1}, \widetilde{D}_1) \cos m\theta + M^{ss}_{nm}(\lambda_{D_1}, \widetilde{D}_1) \sin m\theta\right) \tag{3.16}$$

for $n \neq 0$.

Proof. When D is a circular disk of radius r_0, it is known that (see, for example, [3])

$$\mathcal{K}_D^*[\phi] = \frac{1}{4\pi r_0}\int_{\partial D} \phi \, d\sigma.$$

Since $\partial\widetilde{D}_2$ is a circle and any function belonging to $\mathcal{H}^*(\partial\widetilde{D}_2)$ has a zero mean, $\mathcal{K}^*_{\widetilde{D}_2} = 0$ on $\mathcal{H}^*(\partial\widetilde{D}_2)$. Therefore, we only need to consider the second term in $\widetilde{\mathcal{A}}$. It is easy to see that

$$\mathcal{S}_{\widetilde{D}_2}[\varphi_n^c](r,\theta) = -\frac{\tilde{r}_2^{-n+1}}{2n} r^n \cos n\theta, \tag{3.17}$$

$$\mathcal{S}_{\widetilde{D}_2}[\varphi_n^s](r,\theta) = -\frac{\tilde{r}_2^{-n+1}}{2n} r^n \sin n\theta \tag{3.18}$$

for $0 \le r \le \tilde{r}_2$. Thus, we have

$$\widetilde{\mathcal{A}}[\varphi_n^c](\zeta) = -\frac{\tilde{r}_2^{-n+1}}{2n}\frac{\partial}{\partial \nu_2}\int_{\partial\widetilde{D}_1} G(\zeta,\zeta')\left(\lambda_{D_1} I - \mathcal{K}^*_{\widetilde{D}_1}\right)^{-1}\left[\frac{\partial}{\partial \nu_1}\mathrm{Re}\{P_n\}\right](\zeta')\, d\sigma(\zeta'). \tag{3.19}$$

It is known that [1]

$$G(x,y) = \sum_{m=1}^{\infty} \frac{(-1)}{2\pi m}\frac{\cos(m\theta_x)}{r_x^m} r_y^m \cos(m\theta_y) + \frac{(-1)}{2\pi m}\frac{\sin(m\theta_x)}{r_x^m} r_y^m \sin(m\theta_y), \quad |x| < |y|,$$

where (r_x, θ_x) and (r_y, θ_y) are the polar coordinates of x and y, respectively. Then, by letting $x = \zeta$ and $y = \zeta' \in \partial\widetilde{D}_2$, we get

$$\begin{aligned}\widetilde{\mathcal{A}}[\varphi_n^c](\zeta) = \sum_{m=1}^{\infty} -\frac{\tilde{r}_2^{-(n+m)}}{4\pi n}\cos m\theta \int_{\partial\widetilde{D}_1} \mathrm{Re}\{P_m\}\left(\lambda_{D_1} I - \mathcal{K}^*_{\widetilde{D}_1}\right)^{-1}\left[\frac{\partial}{\partial \nu_1}\mathrm{Re}\{P_n\}\right](\zeta')\, d\sigma(\zeta') \\ - \frac{\tilde{r}_2^{-(n+m)}}{4\pi n}\sin m\theta \int_{\partial\widetilde{D}_1} \mathrm{Im}\{P_m\}\left(\lambda_{D_1} I - \mathcal{K}^*_{\widetilde{D}_1}\right)^{-1}\left[\frac{\partial}{\partial \nu_1}\mathrm{Re}\{P_n\}\right](\zeta')\, d\sigma(\zeta').\end{aligned}$$

Finally, from the definition of the CGPTs (see (2.10)), (3.15) follows. Similarly, one can derive (3.16). ∎

Let us define

$$M_{nm} = M_{nm}(\lambda_{D_1}, \widetilde{D}_1) = \begin{pmatrix} M_{nm}^{cc}(\lambda_{D_1}, \widetilde{D}_1) & M_{nm}^{cs}(\lambda_{D_1}, \widetilde{D}_1) \\ M_{nm}^{sc}(\lambda_{D_1}, \widetilde{D}_1) & M_{nm}^{ss}(\lambda_{D_1}, \widetilde{D}_1) \end{pmatrix}$$

and

$$\widetilde{M}_{nm} = -\frac{\tilde{r}_2^{-(n+m)}}{4\pi n} M_{nm}(\lambda_{D_1}, \widetilde{D}_1). \tag{3.20}$$

In view of Proposition 3.1, we see that the operator $\widetilde{\mathcal{A}}$ can be represented in a block matrix form as follows:

$$\widetilde{\mathcal{A}} = \begin{bmatrix} \widetilde{M}_{11} & \widetilde{M}_{12} & \widetilde{M}_{13} & \cdots \\ \widetilde{M}_{21} & \widetilde{M}_{22} & \cdots & \cdots \\ \widetilde{M}_{31} & \cdots & \cdots & \\ \cdots & & & \end{bmatrix}. \tag{3.21}$$

Recall that $\widetilde{D}_1$ is contained in the disk $\widetilde{B}_1$ with radius $\tilde{r}_1$. One can derive that

$$|M_{nm}(\lambda_{D_1}, \widetilde{D}_1)| \le C\tilde{r}_1^{n+m}$$

for some positive constant C [3]. Therefore,

$$|\widetilde{M}_{nm}(\lambda_{D_1}, \widetilde{D}_1)| \le C\left(\frac{\tilde{r}_1}{\tilde{r}_2}\right)^{n+m}. \tag{3.22}$$

This decay property of $\widetilde{M}_{nm}$ is crucial for our conformal mapping technique. An important consequence is that the operator $\widetilde{\mathcal{A}}$ can be efficiently approximated by finite-dimensional matrices obtained through a standard truncation procedure. Here we remark that $\widetilde{\mathcal{A}} = O((\tilde{r}_1/\tilde{r}_2)^2)$.

If the particle D_1 is in the strong regime, then we may write $d = c\delta$ for some $c > 0$. If c is of order one, the ratio $\frac{\tilde{r}_1}{\tilde{r}_2}$ is relatively small (but regardless of how small δ is). In section 4 we apply the eigenvalue perturbation method to analyze the spectral nature more explicitly when we consider the related inverse problem.

3.5. Spectral decomposition of $\mathcal{A}$ and the scattered field.

It is clear that $\widetilde{\mathcal{A}}$ (or $\mathcal{A}$) is compact. Moreover it can be shown that $\widetilde{\mathcal{A}}$ is self-adjoint in $\mathcal{H}^*(\partial\widetilde{D}_2)$.

Lemma 3.3. *The operator $\widetilde{\mathcal{A}}$ is self-adjoint in $\mathcal{H}^*(\partial\widetilde{D}_2)$, i.e.,*

$$(\widetilde{\phi}, \widetilde{\mathcal{A}}[\widetilde{\psi}])_{\mathcal{H}^*(\partial\widetilde{D}_2)} = (\widetilde{\psi}, \widetilde{\mathcal{A}}[\widetilde{\phi}])_{\mathcal{H}^*(\partial\widetilde{D}_2)}$$

for $\widetilde{\phi}, \widetilde{\psi} \in \mathcal{H}^*(\partial\widetilde{D}_2)$.

Proof. For simplicity, we consider the case when $\widetilde{\phi} = \varphi_m^c$ and $\widetilde{\psi} = \varphi_n^c$ only. The other cases can be done similarly. From (3.17), we have $\mathcal{S}_{\widetilde{D}_2}[\varphi_n^c]|_{\partial\widetilde{D}_2} = -\frac{\tilde{r}_2}{2n}\varphi_n^c$. Then, using (3.20) and (3.21), we have

$$\begin{aligned}(\varphi_n^c, \widetilde{\mathcal{A}}[\varphi_m^c])_{\mathcal{H}^*(\partial\widetilde{D}_2)} &= -(\varphi_n^c, \mathcal{S}_{\partial\widetilde{D}_2}\widetilde{\mathcal{A}}[\varphi_m^c])_{-\frac{1}{2},\frac{1}{2}}\\ &= -\frac{\tilde{r}_2^{-(n+m-1)}}{8nm}M_{nm}(\lambda_{D_1}, \widetilde{D}_1).\end{aligned}$$

So we get the conclusion. ∎

Thus $\widetilde{\mathcal{A}}$ admits the following spectral decomposition:

$$\widetilde{\mathcal{A}} = \sum_{n=1}^{\infty} \lambda_j \widetilde{\psi}_n \otimes \widetilde{\psi}_n,$$

where $\{(\lambda_n, \widetilde{\psi}_n) : n \ge 1\}$ is the set of its eigenvalue-eigenfunction pairs. We order the eigenvalues in such a way that $|\lambda_j|$ is decreasing and tends to 0 as $j \to \infty$. We remark that all the eigenvalues $\{\lambda_j : j \ge 1\}$ lie in the interval $(-1/2, 1/2)$. Moreover, they can be numerically approximated by the eigenvalues of a finite truncation of the infinite matrix $\widetilde{\mathcal{A}}$.

Thanks to (3.14), if we let $\psi_n = \widetilde{\psi}_n \circ \Phi$, then we obtain

$$\mathcal{A} = \sum_{n=1}^{\infty} \lambda_j \psi_n \otimes \psi_n. \tag{3.23}$$

It is also worth mentioning that the orthogonality of basis $\{\psi_n\}$ is also preserved.

Using the spectral representation formula (3.23), we can derive the following result.

Theorem 3.1. *Assume that Condition 1 holds and that D_2 is in the strong interaction regime. Then the scattered field $u^s_{D_2} = u - u_{D_1}$ by the plasmonic particle D_2 has the following representation:*

$$u^s_{D_2} = \mathcal{S}_{D_2,D_1}[\psi],$$

where ψ satisfies

$$\psi = \sum_{j=1}^{\infty} \frac{(\nabla u^i(z)\cdot \nu, \psi_j)_{\mathcal{H}^*(\partial D_2)}\, \psi_j + O(\delta^2)}{\lambda_{D_2} - \lambda_j}.$$

As a corollary, we obtain the following asymptotic expansion of the scattered field $u - u^i$.

Theorem 3.2. *The following far-field expansion holds:*

$$(u-u^i)(x) = \nabla u^i(z)\cdot M(\lambda_{D_1},\lambda_{D_2},D_1,D_2)\nabla G(x,z) + O\left(\frac{\delta^3}{\mathrm{dist}(\lambda_{D_2},\sigma(\mathcal{A}))}\frac{1}{|x|^2}\right),$$

as $|x|\to\infty$. Here, z is the center of mass of D_2 and $M(\lambda_{D_1},\lambda_{D_2},D_1,D_2)$ is the polarization tensor satisfying

$$M(\lambda_{D_1},\lambda_{D_2},D_1,D_2)_{l,m} = \sum_{j=1}^{\infty} \frac{(\nu_l,\psi_j)_{\mathcal{H}^*(\partial D_2)}(\psi_j, x_m)_{-\frac{1}{2},\frac{1}{2}} + O(\delta^2)}{\lambda_{D_2} - \lambda_j} \tag{3.24}$$

for $l,m = 1,2$.

We can introduce the resonant frequency ω_j for the system of two particles $D_1 \cup D_2$ as in subsection 2.4. From the above far-field expansion of the scattered field, it is clear that when we vary the frequency ω, at certain frequency ω such that $\lambda_{D_2}(\omega) \approx \lambda_j$ for some j which satisfies the condition that

$$(\nu_l,\psi_j)_{\mathcal{H}^*(\partial D_2)}(\psi_j, x_m)_{-\frac{1}{2},\frac{1}{2}} \neq 0,$$

the scattered field will show a sharp peak, which corresponds to the excitation of a plasmonic resonance. Such a frequency is called the (plasmonic) resonant frequency for the system of two particles, which is different from that for the single plasmonic particle D_2. The difference is called the shift of resonant frequency. This shift is due to the interaction of the target particle with the plasmonic particle. As discussed in subsection 2.4, the resonant frequencies ω_j of the two-particle system can also be measured from the far field. They also determine λ_j, which are eigenvalues of the operator $\mathcal{A}$. In the next section, we discuss how to reconstruct the shape of D_1 from these recovered eigenvalues.

4. The inverse problem.

In this section, we discuss the inverse problem to reconstruct the shape of the small unknown particle D_1 by using the resonances of the plasmonic particle D_2 which interacts with D_1. We assume the location of D_1 and the permittivity ε_1 are known for simplicity. As explained in the previous section, we can measure the eigenvalues λ_j for $j = 1,2,\ldots,J$ from the far-field measurements. Since the single set of the measurement data is not enough for the reconstruction, we shall make measurements for many different configurations of the two-particle system. In subsection 4.1, we show how the CGPTs of the unknown particle $\widetilde{D}_1$ can be reconstructed from the measurements of λ_j. In subsection 4.2, we explain the optimal control algorithm to recover the shape of $\widetilde{D}_1$ from the CGPTs. In this way, we reconstruct the transformed shape $\widetilde{D}_1$ first. Once we find $\widetilde{D}_1$, the original shape of D_1 can be easily recovered by using the mapping Φ. In subsection 4.3, we provide several numerical examples.

4.1. Reconstruction of CGPTs. In this subsection, we propose an algorithm to reconstruct the CGPTs from measurements of the eigenvalues λ_j. For ease of presentation, we only consider the first two largest eigenvalues, λ_1 and λ_2. We denote their measurements by $\mathcal{P}_1$ and $\mathcal{P}_2$, respectively. Note that a single measurement of $(\mathcal{P}_1, \mathcal{P}_2)$ typically yields very poor reconstruction of the CGPTs due to the lack of information. To overcome this issue, we need to measure the eigenvalues for different configurations of the two particles. Recall that the target particle contains the origin. We can rotate it around the origin multiple times and measure $(\mathcal{P}_1, \mathcal{P}_2)$ for each configuration. The CGPTs for the target particle after each rotation are related in the following way.

Define

$$N^{(1)}_{m,n}(\lambda, D) = (M^{cc}_{m,n} - M^{ss}_{m,n}) + i(M^{cs}_{m,n} + M^{sc}_{m,n}),$$
$$N^{(2)}_{m,n}(\lambda, D) = (M^{cc}_{m,n} + M^{ss}_{m,n}) + i(M^{cs}_{m,n} - M^{sc}_{m,n})$$

and let $R_\theta D = \{e^{i\theta}x : x \in D\}, \theta \in [0, 2\pi)$. Then for all integers m, n and all angle parameters θ, we have [1]

$$N^{(1)}_{m,n}(R_\theta D) = e^{i(n+m)\theta} N^{(1)}_{m,n}(D), \quad N^{(2)}_{m,n}(R_\theta D) = e^{i(n-m)\theta} N^{(2)}_{m,n}(D).$$

Let us write $d = c\delta$ for some $c > 0$. As discussed in subsection 3.2, if c is of order one, then the deformation of the shape $\widetilde{D}_1$ from D_1 is not so strong. So, if the domain D_1 is rotated by an angle θ, then the transformed domain will also be rotated by the same amount. So we may (approximately) identify $\widetilde{R_\theta D_1}$ with $R_\theta \widetilde{D}_1$.

Measuring $\mathcal{P}_j$ for multiple rotation angles θ_i for $R_\theta \widetilde{D}_1$ will yield a nonlinear system of equations that will allow the recovery of the CGPTs associated with $\widetilde{D}_1$. From the recovered CGPTs, we will reconstruct the shape of $\widetilde{D}_1$. Here, we only consider the shape reconstruction problem. Nevertheless, by using the CGPTs associated with $\widetilde{D}_1$, it is possible to reconstruct the permittivity ε_1 of $\widetilde{D}_1$ in the case it is not a priori given [1].

In view of (3.21) and (3.22), using a standard perturbation method, the asymptotic expansion of the eigenvalue $\lambda_j, j = 1, 2$, is given by

$$\lambda_j = \lambda_j^0 + \lambda_j^1 + \lambda_j^2 + \cdots, \quad \text{where } \lambda_j^k = O\big((\tilde{r}_1/\tilde{r}_2)^{k+2} \big). \tag{4.1}$$

Each term on the right-hand side of the above expansion can be computed explicitly. Although we omit the explicit expressions, we mention that they are nonlinear and depend on CGPTs in the following way:

$$\begin{aligned}
\lambda_j^0 &= \lambda_j^0(M_{11}),\\
\lambda_j^1 &= \lambda_j^1(M_{11}, M_{12}),\\
\lambda_j^2 &= \lambda_j^2(M_{11}, M_{12}, M_{22}, M_{13}),\\
\vdots &= \qquad \vdots\\
\lambda_j^k &= \lambda_j^k(\cup_{m+n\le k+2}\{M_{mn}\}).
\end{aligned}$$

Suppose we have measurements $\mathcal{P}_1(\theta)$ and $\mathcal{P}_2(\theta)$ for 11 different rotation angles $\theta_1, \theta_2, \dots, \theta_{11}$ of the unknown particle $\widetilde{D}_1$. We can reconstruct M_{nm} approximately for $m+n \le 5$. Recall that $M_{mn} = M_{nm}^{\intercal}$. We look for a set of matrices $\{M_{nm}^{(1)}\}_{m+n\le 5}$ satisfying $[M_{nm}^{(1)}]^{\intercal} = M_{mn}^{(1)}$ and the following nonlinear system: for $j = 1, 2$,

$$\begin{aligned}
\mathcal{P}_j(\theta_1) &= \sum_{l=0}^{3} \lambda_j^l\Big(\cup_{m+n\le l+2}\, \{M_{nm}^{(1)}(R_{\theta_1}\widetilde{D}_1)\}\Big),\\
\mathcal{P}_j(\theta_2) &= \sum_{l=0}^{3} \lambda_j^l\Big(\cup_{m+n\le l+2}\, \{M_{nm}^{(1)}(R_{\theta_2}\widetilde{D}_1)\}\Big),\\
\vdots \quad &= \qquad\qquad \vdots\\
\mathcal{P}_j(\theta_{11}) &= \sum_{l=0}^{3} \lambda_j^l\Big(\cup_{m+n\le l+2}\, \{M_{nm}^{(1)}(R_{\theta_{11}}\widetilde{D}_1)\}\Big).
\end{aligned}$$

We note that the above equations have 22 independent parameters. They can be solved by using standard optimization methods. We expect that

$$M_{nm} = M_{nm}^{(1)} + O\big((\tilde{r}_1/\tilde{r}_2)^6 \big) \quad \text{for } m+n \le 5.$$

The above scheme can be easily generalized to reconstruct the higher order CGPTs M_{nm}. This requires more measurement data $(\mathcal{P}_1, \mathcal{P}_2)$ from more rotations. Let $k \ge 2$. One can see that (using the symmetry $[M_{nm}^{(k)}]^{\intercal} = M_{mn}^{(k)}$) the set of GPTs M_{mn} satisfying $m+n \le 4k+1$ contains e_k independent parameters, where e_k is given by

$$e_k = 16k^2 + 6k.$$

Therefore, we need $e_k/2$ pairs of $(\mathcal{P}_1, \mathcal{P}_2)$ to reconstruct these GPTs. Let $\{M_{nm}^{(k)}\}_{m+n\le 4k+1}$ be the set of matrices satisfying $[M_{nm}^{(k)}]^{\intercal} = M_{mn}^{(k)}$ and the following system of equations:

$$\mathcal{P}_j(\theta_i) = \sum_{l=0}^{k-1} \lambda_j^l\Big(\cup_{m+n\le l+2}\, \{M_{nm}^{(k)}(R_{\theta_i}\widetilde{D}_1)\}\Big), \quad i = 1, \dots, e_k,\ j = 1, 2.$$

Then we have

$$M_{nm} = M_{nm}^{(k)} + O\big((\tilde{r}_1/\tilde{r}_2)^{4k+2} \big) \quad \text{for } m+n \le 4k+1.$$

4.2. Optimal control approach. Now, in order to recover the shape of $\widetilde{D}_1$ from the CGPTs M_{mn}, we can minimize the energy functional

$$\mathcal{J}_c^{(l)}[B] := \frac{1}{2} \sum_{H,F\in\{c,s\}} \sum_{n+m\leq k} \left| M_{mn}^{HF}(\lambda_{D_1}, B) - M_{mn}^{HF}(\lambda_{D_1}, \widetilde{D}_1) \right|^2 . \tag{4.2}$$

We apply the gradient descent method for the minimization. We need the shape derivative of the functional $\mathcal{J}_c^{(l)}[B]$. For a small $\eta > 0$, let B_η be an η-deformation of B; i.e., there is a scalar function $h \in \mathcal{C}^1(\partial B)$, such that

$$\partial B_\eta := \{x + \eta h(x)\nu(x) \ : x \in \partial B\}.$$

According to [1, 2, 5], the perturbation of the CGPTs due to the shape deformation is given by

$$\begin{aligned} &M_{nm}^{HF}(\lambda_{D_1}, B_\eta) - M_{nm}^{HF}(\lambda_{D_1}, B) \\ &\quad = \eta(k_{\lambda_{D_1}} - 1) \int_{\partial B} h(x) \left[\frac{\partial u}{\partial \nu}\Big|_- \frac{\partial v}{\partial \nu}\Big|_- + \frac{1}{k_{\lambda_{D_1}}} \frac{\partial u}{\partial T}\Big|_- \frac{\partial v}{\partial T}\Big|_- \right](x)\, d\sigma(x) + O(\eta^2), \end{aligned} \tag{4.3}$$

where

$$k_{\lambda_{D_1}} = (2\lambda_{D_1} + 1)/(2\lambda_{D_1} - 1), \tag{4.4}$$

and u and v are, respectively, the solutions to the following transmission problems:

$$\begin{cases} \Delta u = 0 & \text{in } B \cup (\mathbb{R}^2 \backslash \overline{B}) , \\ u|_+ - u|_- = 0 & \text{on } \partial B , \\ \dfrac{\partial u}{\partial \nu}\Big|_+ - k_{\lambda_{D_1}} \dfrac{\partial u}{\partial \nu}\Big|_- = 0 & \text{on } \partial B , \\ (u - H)(x) = O(|x|^{-1}) & \text{as } |x| \to \infty \end{cases} \tag{4.5}$$

and

$$\begin{cases} \Delta v = 0 & \text{in } B \cup (\mathbb{R}^2 \backslash \overline{B}) , \\ k_{\lambda_{D_1}} v|_+ - v|_- = 0 & \text{on } \partial B , \\ \dfrac{\partial v}{\partial \nu}\Big|_+ - \dfrac{\partial v}{\partial \nu}\Big|_- = 0 & \text{on } \partial B , \\ (v - F)(x) = O(|x|^{-1}) & \text{as } |x| \to \infty . \end{cases} \tag{4.6}$$

Here, $\partial/\partial T$ is the tangential derivative. In the case of M_{nm}^{cs}, for example, we put $H = \mathrm{Re}\{P_n\} = r^n \cos n\theta$ and $F = \mathrm{Im}\{P_m\} = r^n \sin n\theta$. The other cases can be handled similarly.

Let

$$w_{m,n}^{HF}(x) = (k_{\lambda_{D_1}} - 1) \left[\frac{\partial u}{\partial \nu}\Big|_- \frac{\partial v}{\partial \nu}\Big|_- + \frac{1}{k_{\lambda_{D_1}}} \frac{\partial u}{\partial T}\Big|_- \frac{\partial v}{\partial T}\Big|_- \right](x), \quad x \in \partial B .$$

The shape derivative of $\mathcal{J}_c^{(l)}$ at B in the direction of h is given by

$$\langle d_S \mathcal{J}_c^{(l)}[B], h\rangle = \sum_{H,F\in\{c,s\}} \sum_{m+n\le k} \delta_N^{HF} \langle w_{m,n}^{HF}, h\rangle_{L^2(\partial B)} ,$$

where

$$\delta_N^{HF} = M_{nm}^{HF}(\lambda_{D_1}, B) - M_{nm}^{HF}(\lambda_{D_1}, \widetilde{D}_1) .$$

By using the shape derivatives of the CGPTs, we can get an approximation for the matrix $\big(\widetilde{M}_{nm}(\lambda_{D_1}, B_\eta)\big)_{n,m=1}^N$ for the slightly deformed shape. Next, the shape derivative of $\lambda_j^N(B)$ can be computed by using the standard eigenvalue perturbation theory. Finally, by applying a gradient descent algorithm, we can minimize, at least locally, the energy functional $\mathcal{J}_c^{(l)}$. Then we get the shape of the original particle D_1 using $D_1 = \Phi^{-1}(\widetilde{D}_1)$.

4.3. Numerical examples. In this subsection, we support our theoretical results by numerical examples. In what follows, we set $\delta = 0.001$. We also assume that B_1 and B_2 are disks of radii $r_1 = \delta$ and $r_2 = 1$, respectively, and they are separated by a distance $d = 5\delta$. Then the ratio $\tilde{r}_1/\tilde{r}_2$ between the transformed radii is approximately 0.127. Note that the ratio is rather small but much larger than the small parameter δ. We suppose that the material parameter ε_1 of D_1 is known and to be given by $\varepsilon_1 = 3$, and so it holds that $\lambda_{D_1} = 1$.

We rotate the unknown particle D_1 by the angle θ_i, $i = 1, 2, \ldots, 11$, and get the measurement pair $(\mathcal{P}_1(\theta_i), \mathcal{P}_2(\theta_i))$ for each rotation θ_i, where θ_i is given by

$$\theta_i = \frac{2\pi}{11}(i-1), \quad i = 1, 2, \ldots, 11.$$

We mention that, as discussed in [9], we can measure $(\mathcal{P}_1, \mathcal{P}_2)$ from the local peaks of the plasmonic resonant far field.

Figure 3 shows the shift in the plasmonic resonance. In the absence of the dielectric particle D_1, the local peak occurs only at $\lambda_{D_2} = 0$. If the particle D_1 is presented in a strong regime, then many local peaks appear. By measuring the first two largest values of λ_{D_2} at which a local peak appears, we get $(\mathcal{P}_1, \mathcal{P}_2)$ approximately.

From measurements of $(\mathcal{P}_1, \mathcal{P}_2)$, we recover the contracted GPTs using the algorithm described in subsection 4.1. We then minimize functional (4.2) to reconstruct an approximation of $\widetilde{D}_1$. Finally, we use $D_1 = \Phi^{-1}(\widetilde{D}_1)$ to get the shape of D_1. We consider the case of D_1 being a flower-shaped particle and show comparison between the target shapes and the reconstructed ones, as shown in Figure 4. We recover the first contracted GPTs up to order 5, i.e., M_{mn} for $m + n \le 5$. We take as an initial guess the equivalent ellipse to $\widetilde{D}_1$, determined from the recovered first order polarization tensor. The required number of iterations is 30. It is clear that they are in good agreement.

5. Conclusion. In this paper, we have made the mathematical foundation of near-field sensing complete. We have considered the sensing of a small target particle using a plasmonic particle in the strong interaction regime, where the distance between the two particles is comparable to the small size of the target particle. We have introduced a conformal mapping which transforms the two-particle system into a shell-core structure, in which the inner dielectric core corresponds to the target object. Then we have analyzed the shift in the resonance

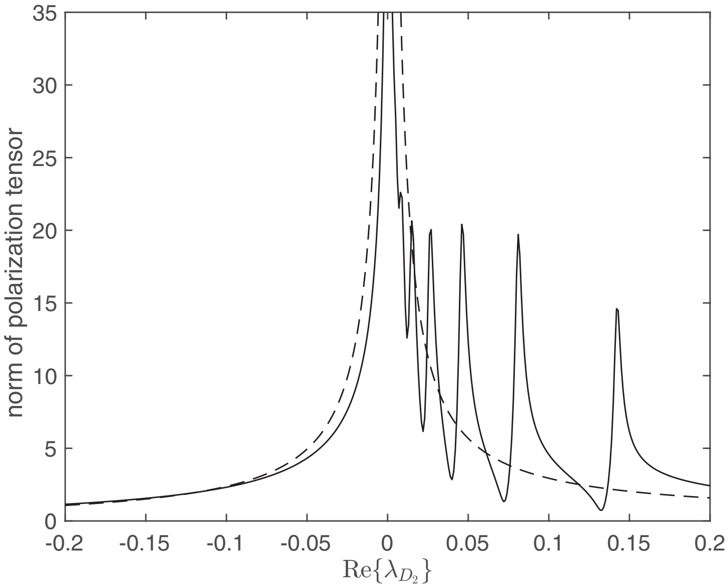

Figure 3. *The magnitude of the polarization tensor. The dotted line (resp., solid line) represents the case when the dielectric particle D_1 is absent (resp., present). We set* $\mathrm{Im}\{\lambda_2\} = 0.003$.

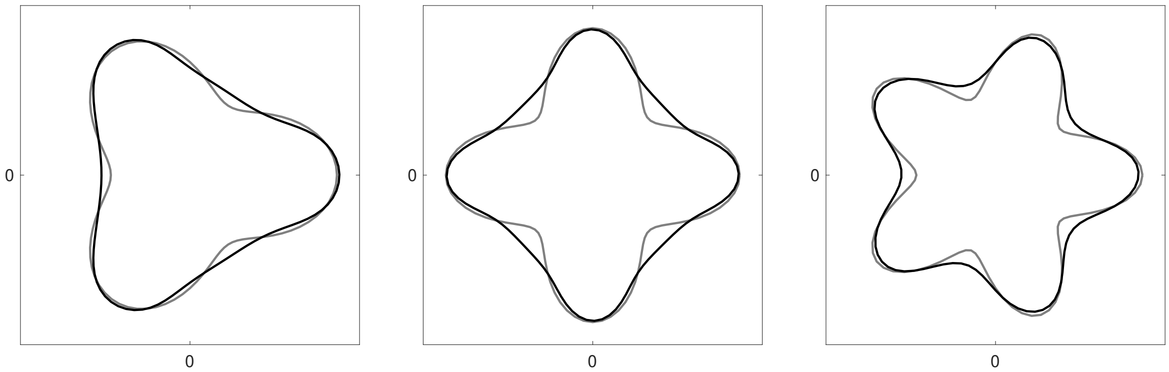

Figure 4. *Comparison between the original shape (gray) of the particle D_1 and the reconstructed one (black). The iteration number is* 30.

frequencies due to the presence of the inner dielectric core. We have shown that this shift encodes information on the contracted polarization tensors of the core, from which one can reconstruct its shape, and hence the target object. It is worth mentioning that although we considered only the two-dimensional case in this paper, our conformal mapping approach can be extended to the three-dimensional case. Although the Laplacian is not preserved in 3D, there is a nice way to overcome this difficulty [27]. The extension to the 3D case will be the subject of a forthcoming paper.

REFERENCES

[1] H. Ammari, J. Garnier, W. Jing, H. Kang, M. Lim, K. Sølna, and H. Wang, *Mathematical and Statistical Methods for Multistatic Imaging*, Lecture Notes in Math. 2098, Springer, Cham, 2013.

[2] H. Ammari, J. Garnier, H. Kang, M. Lim, and S. Yu, *Generalized polarization tensors for shape description*, Numer. Math., 126 (2014), pp. 199–224.

[3] H. Ammari and H. Kang, *Polarization and Moment Tensors with Applications to Inverse Problems and Effective Medium Theory*, Appl. Math. Sci. 162, Springer-Verlag, New York, 2007.

[4] H. Ammari and H. Kang, *Generalized polarization tensors, inverse conductivity problems, and dilute composite materials: A review*, in Inverse Problems, Multi-scale Analysis and Effective Medium, Contemp. Math. 408, AMS, Providence, RI, 2006, pp. 1–67.

[5] H. Ammari, H. Kang, M. Lim, and H. Zribi, *The generalized polarization tensors for resolved imaging. Part* I: *Shape reconstruction of a conductivity inclusion*, Math. Comp., 81 (2012), pp. 367–386.

[6] H. Ammari and A. Khelifi, *Electromagnetic scattering by small dielectric inhomogeneities*, J. Math. Pures Appl. (9), 82 (2003), pp. 749–842.

[7] H. Ammari, P. Millien, M. Ruiz, and H. Zhang, *Mathematical analysis of plasmonic nanoparticles: The scalar case*, Arch. Ration. Mech. Anal., 224 (2017), pp. 597–658.

[8] H. Ammari, M. Ruiz, S. Yu, and H. Zhang, *Mathematical analysis of plasmonic resonances for nanoparticles: The full Maxwell equations*, J. Differential Equations, 261 (2016), pp. 3615–3669.

[9] H. Ammari, M. Ruiz, S. Yu, and H. Zhang, *Reconstructing fine details of small objects by using plasmonic spectroscopic data*, SIAM J. Imaging Sci., 11 (2018), pp. 1–23, https://doi.org/10.1137/17M1126540.

[10] H. Ammari and H. Zhang, *A mathematical theory of super-resolution by using a system of subwavelength Helmholtz resonators*, Comm. Math. Phys., 337 (2015), pp. 379–428.

[11] H. Ammari and H. Zhang, *Super-resolution in high contrast media*, Proc. Royal Soc. A, 471 (2015), 20140946.

[12] H. Ammari and H. Zhang, *Effective medium theory for acoustic waves in bubbly fluids near Minnaert resonant frequency*, SIAM J. Math. Anal., 49 (2017), pp. 3252–3276, https://doi.org/10.1137/16M1078574.

[13] K. Ando and H. Kang, *Analysis of plasmon resonance on smooth domains using spectral properties of the Neumann-Poincaré operator*, J. Math. Anal. Appl., 435 (2016), pp. 162–178.

[14] J.N. Anker, W.P. Hall, O. Lyandres, N.C. Shah, J. Zhao, and R.P. Van Duyne, *Biosensing with plasmonic nanosensors*, Nature Material, 7 (2008), pp. 442–453.

[15] E. Bonnetier and F. Triki, *On the spectrum of the Poincaré variational problem for two close-to-touching inclusions in* 2*D*, Arch. Rational Mech. Anal., 209 (2013), pp. 541–567.

[16] E. Bonnetier and F. Triki, *Pointwise bounds on the gradient and the spectrum of the Neumann-Poincaré operator: The case of* 2 *discs*, in Multi-scale and High-Contrast PDE: From Modelling, to Mathematical Analysis, to Inversion, Contemp. Math. 577, AMS, Providence, RI, 2012, pp. 81–92.

[17] C. Ciraci et al., *Probing the ultimate limits of plasmonic enhancement*, Science, 337 (2012), pp. 1072–1074.

[18] K.L. Kelly, E. Coronado, L.L. Zhao, and G.C. Schatz, *The optical properties of metal nanoparticles: The influence of size, shape, and dielectric environment*, J. Phys. Chem. B, 107 (2003), pp. 668–677.

[19] J.B. Keller, *A theorem on the conductivity of a composite medium*, J. Math. Phys., 5 (1964), 548.

[20] C. Kittel, *Introduction to Solid State Physics*, 8th ed., Wiley & Sons, 2004.

[21] S. Link and M.A. El-Sayed, *Shape and size dependence of radiative, non-radiative and photothermal properties of gold nanocrystals*, Int. Rev. Phys. Chem., 19 (2000), pp. 409–453.

[22] J.B. Pendry, A. Aubry, D.R. Smith, and S.A. Maier, *Transformation optics and subwavelength control of light*, Science, 337 (2012), pp. 549–552.

[23] J.B. Pendry, Y. Luo, and R. Zhao, *Transforming the optical landscape*, Science, 348 (2015), pp. 521–524.

[24] J.B. Pendry, A.I. Fernandez-Dominguez, Y. Luo, and R. Zhao, *Capturing photons with transformation optics*, Nature Phys., 9 (2013), pp. 518–522.

[25] L.B. Scaffardi and J.O. Tocho, *Size dependence of refractive index of gold nanoparticles*, Nanotech.,

17 (2006), pp. 1309–1315.
[26] M.S. Vogelius and D. Volkov, *Asymptotic formulas for perturbations in the electromagnetic fields due to the presence of inhomogeneities of small diameter*, M2AN Math. Model. Numer. Anal., 34 (2000), pp. 723–748.
[27] S. Yu and H. Ammari, *Plasmonic interaction between nanospheres*, SIAM Rev., 60 (2018), pp. 356–385, https://doi.org/10.1137/17M1115319.